

## Influence of prior plastic deformation on the thermal-martensitic-transformation in an Fe-Ni-Al alloy

N. JOST, E. HORNBOKEN

*Institute of Materials, Ruhr-University Bochum, D-4630 Bochum, FRG*

It is well known that the temperatures of martensitic transformation are not only determined by the chemical composition of an alloy. Lattice defects and other elements of the microstructure, which act as hardening-mechanisms, also have strong effects.

In principle, hardening of the parent phase (i.e. the austenite) impedes the subsequent martensitic growth and may, thereby, lead to a decrease of  $M_s$  because of an increasing undercooling,  $\Delta T$ , below the thermodynamical equilibrium temperature,  $T_0$  [1, 2]

$$M_s = T_0 - \Delta T \quad (1)$$

The four principle hardening-mechanisms are derived from zero- to three-dimensional obstacles [3]: 0, point defect (solid solution-, radiation hardening); 1, dislocations (work hardening); 2, grain boundaries (fine grain hardening); 3, precipitates (precipitation-, dispersion hardening). The zero- to two-dimensional defects influence the undercooling  $\Delta T$ . Precipitation also changes the chemical composition of the matrix and thus  $T_0$ .

Differences of opinion exist in the understanding of the effects of dislocation-substructures on a subsequent martensitic transformation [4-6]. Therefore, it is useful to study the transformation behaviour after prior plastic deformation by taking into consideration nucleation and growth of the martensite.

In this work a metastable Fe-31 Ni-4 Al alloy (wt %) with  $M_s = -151^\circ\text{C}$  was deformed by rolling between 0 and 50% reduction in thickness,  $\epsilon$ , in steps of  $\epsilon = 10\%$  at room-temperature (RT) and  $300^\circ\text{C}$ . By X-ray diffractometry it could be verified that no strain-induced martensite was formed. In order to characterize the  $M_s$  temperature, dilatometric studies were applied in the temperature range between RT

and liquid-nitrogen temperature ( $-196^\circ\text{C}$ ). The microstructures before and after deformation and transformation were analysed by light- and transmission electron microscopy. Fig. 1a shows the initial, undeformed and untransformed austenitic microstructure. Cooling this state to  $-196^\circ\text{C}$  produces martensite with a characteristic, midribbed lenticular morphology (Fig. 1b). Nucleation sites for the transformation are grain boundaries and subsequently martensite-austenite interfaces. If the material is highly deformed by cold rolling ( $T_c = \text{RT}$ ,  $\epsilon > 30\%$ ) shear bands arise [7] (Fig. 2a). They affect the subsequent martensitic transformation by undercooling in two ways (Fig. 2b): (1) the shear bands generate new additional martensite nucleation sites; (2) the structural discontinuity by the shear bands impedes the growth of martensite crystals in length and thickness. This, in turn, leads to a lath-like martensite morphology.

The influence of prior plastic deformation on the  $M_s$  temperature and on the microhardness of the austenite and martensite is shown in Fig. 3. In the case of cold-rolling, a decrease of  $M_s$  up to about  $\epsilon = 20\%$  is followed by an increase of  $M_s$  at higher amounts of deformation. At about  $\epsilon = 20\%$  the work hardening of austenite also increased strongly. On the other hand, deformation at  $300^\circ\text{C}$  leads to a steady decrease in  $M_s$  and to an equally steady increase in austenite hardness. In all cases the martensite hardness amounts to about  $520 H_v 0.01$ . This can be explained by transmission electron micrographs of the martensite substructure after different amounts of deformation (i.e. lenticular and lath martensite) (Fig. 4). In all cases two principle deformation characteristics can be detected together: (1) a high density of micro-twins, which

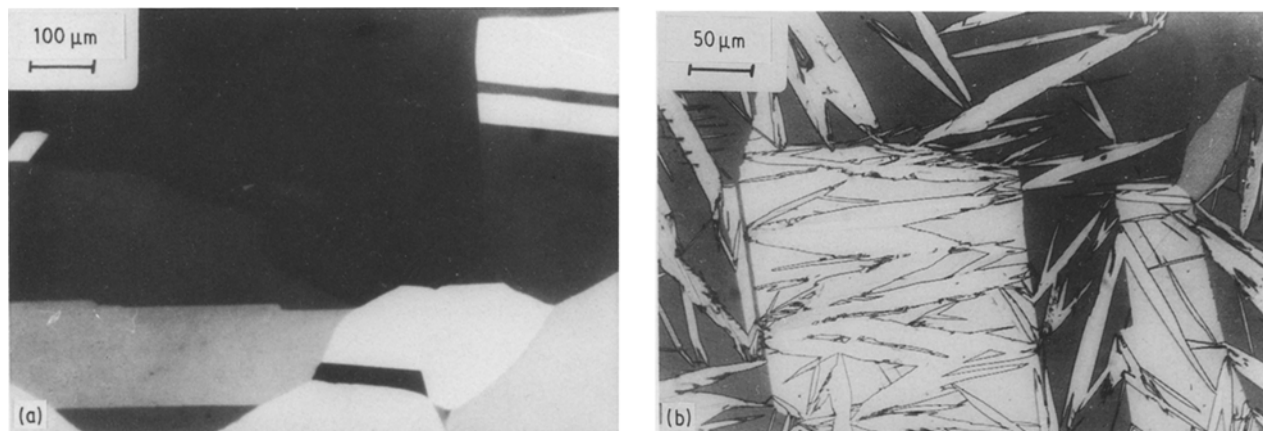


Figure 1 (a) Undeformed and untransformed austenite (light microscopy). (b) Undeformed austenite after cooling to  $-196^\circ\text{C}$ , martensite plates with lenticular morphology (light microscopy).

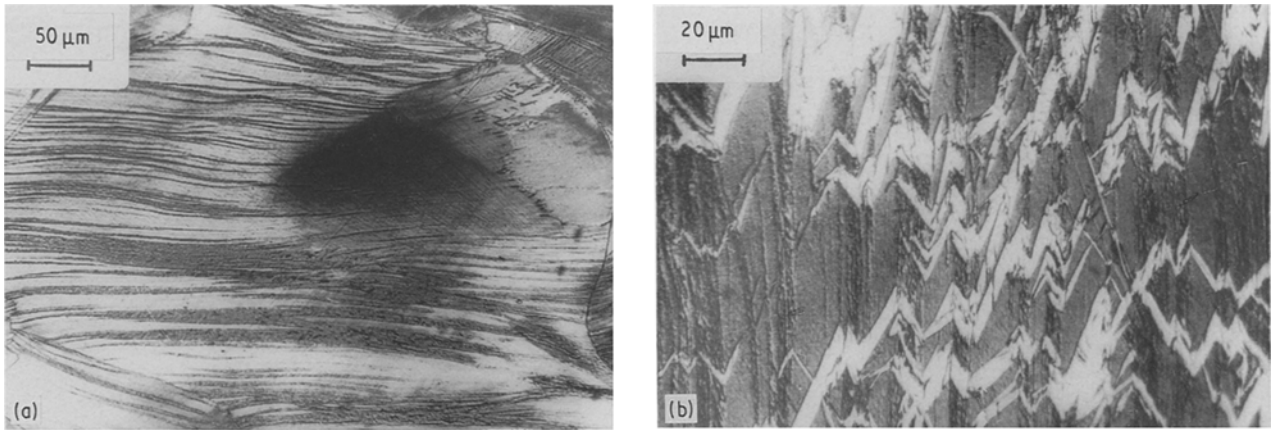


Figure 2 (a) Austenite after high degrees of deformation ( $\epsilon = 50\%$ ,  $T_\epsilon = RT$ ), building of large shear bands (light microscopy). (b) Deformed austenite after cooling to  $-196^\circ\text{C}$ , shear bands generate new additional martensite nucleation sites (light microscopy).

result from lattice deformation by twinning; (2a) dislocations, which were induced by transformation-slip at low amounts of deformation; (2b) dislocations, which were evidently inherited from the deformed austenite at higher amounts of deformation.

Fig. 5 shows transmission electron micrographs of the deformed and untransformed austenite. In agreement with Figs 2 and 3 it can be shown that cold-rolling favours the formation of inhomogeneous dislocation substructures. Deformation at  $300^\circ\text{C}$  leads to a much more homogeneous dislocation substructure. A very homogeneous dislocation substructure of the austenite may be received with higher deformation temperatures ( $T_\epsilon > 300^\circ\text{C}$ ) and higher amounts of deformation ( $\epsilon > 50\%$ ). As a result of such a microstructure, a strong increase of  $\Delta T$ , and thereby a decrease in  $M_s$ , can be supposed and the martensite

microstructure may change from internal twins with dislocations to a pure dislocation substructure.

This study confirms that a homogeneous dislocation hardening of the austenite can depress the  $M_s$  temperature considerably, because of the increasing undercooling  $\Delta T$ . Highly localized deformation such as slip- and especially shear bands can aid nucleation and therefore increase  $M_s$ . They will also impede propagation of martensite crystals. The course of  $M_s$  with bulk amount of plastic deformation is the more ambiguous the higher is the heterogeneity of the deformation microstructure. Therefore the undercooling,  $\Delta T$ , in Equation 1 as a function of the amount of deformation can be divided into two terms:

$$\Delta T(\epsilon) = \Delta T_H - \Delta T_N \quad (2)$$

from which  $\Delta T_H$  describes the effect of a homogeneous distribution of dislocations.  $\Delta T_N$  is the undercooling, influenced by an inhomogeneous distribution of dislocations in shear bands (i.e. nucleation sites). The effect of hardening mechanisms, which are independent of plastic deformation, such as radiation hardening or fine-grain hardening can be added up in  $\Delta T_{\epsilon=0}$

$$M_s = T_0 - (\Delta T_{\epsilon=0} + \Delta T_H - \Delta T_N) \quad (3)$$

The change of  $M_s$  as a function of the amount of plastic deformation can now be formulated as follows:

$$\frac{dM_s}{d\epsilon} = \frac{dT_0}{d\epsilon} - \frac{d\Delta T_{\epsilon=0}}{d\epsilon} - \frac{d\Delta T_H}{d\epsilon} + \frac{d\Delta T_N}{d\epsilon}$$

$$\frac{dM_s}{d\epsilon} = - \frac{d\Delta T_H}{d\epsilon} + \frac{d\Delta T_N}{d\epsilon} \quad (4)$$

The first term is proportional to the dislocation density  $GbN^{1/2}$  and, thereby, to the yield strength  $\tau_y$ . For this term a total differential can be formulated, whereas the influence of shear bands on the introduction of internal stresses,  $\bar{\tau}_i$ , is not yet clear. This could be explained by further investigation of the structure of the shear bands:

$$\frac{dM_s}{d\epsilon} = - \frac{\partial \Delta T_H}{\partial \tau_y} \frac{\delta \tau_y}{\delta \epsilon} + \frac{d\Delta T_N}{d\epsilon} \quad (5)$$

The sum may be positive or negative, depending on the dislocation structure and on the amount of plastic deformation.

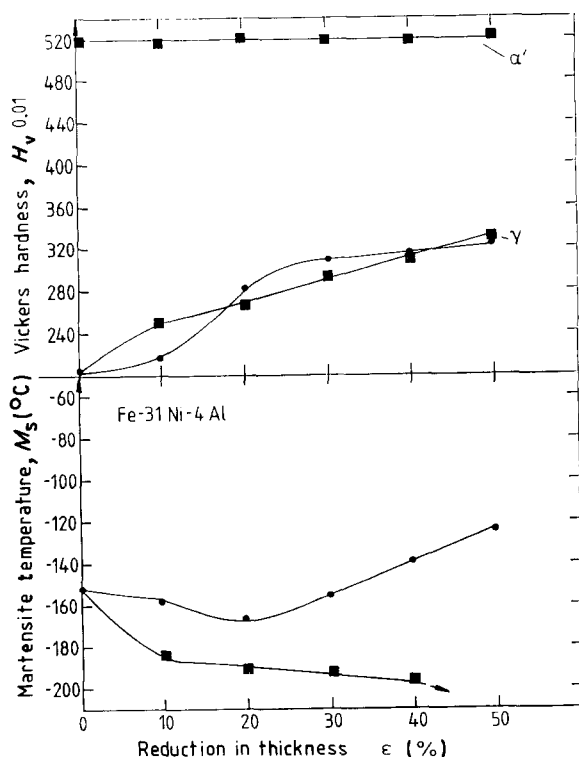


Figure 3 The effect of prior deformation on the microhardness of the austenite and martensite and on the  $M_s$  temperature. (●)  $T_\epsilon = RT$ ; (■)  $T_\epsilon = 300^\circ\text{C}$ .

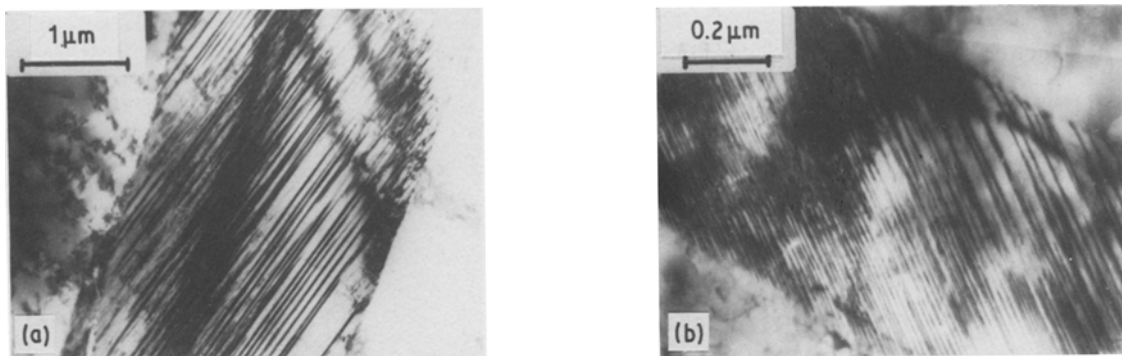


Figure 4 (a) Martensite substructure after low amounts of deformation (lenticular martensite) (TEM). (b) Martensite substructure after high amounts of deformation (lath martensite) (TEM).

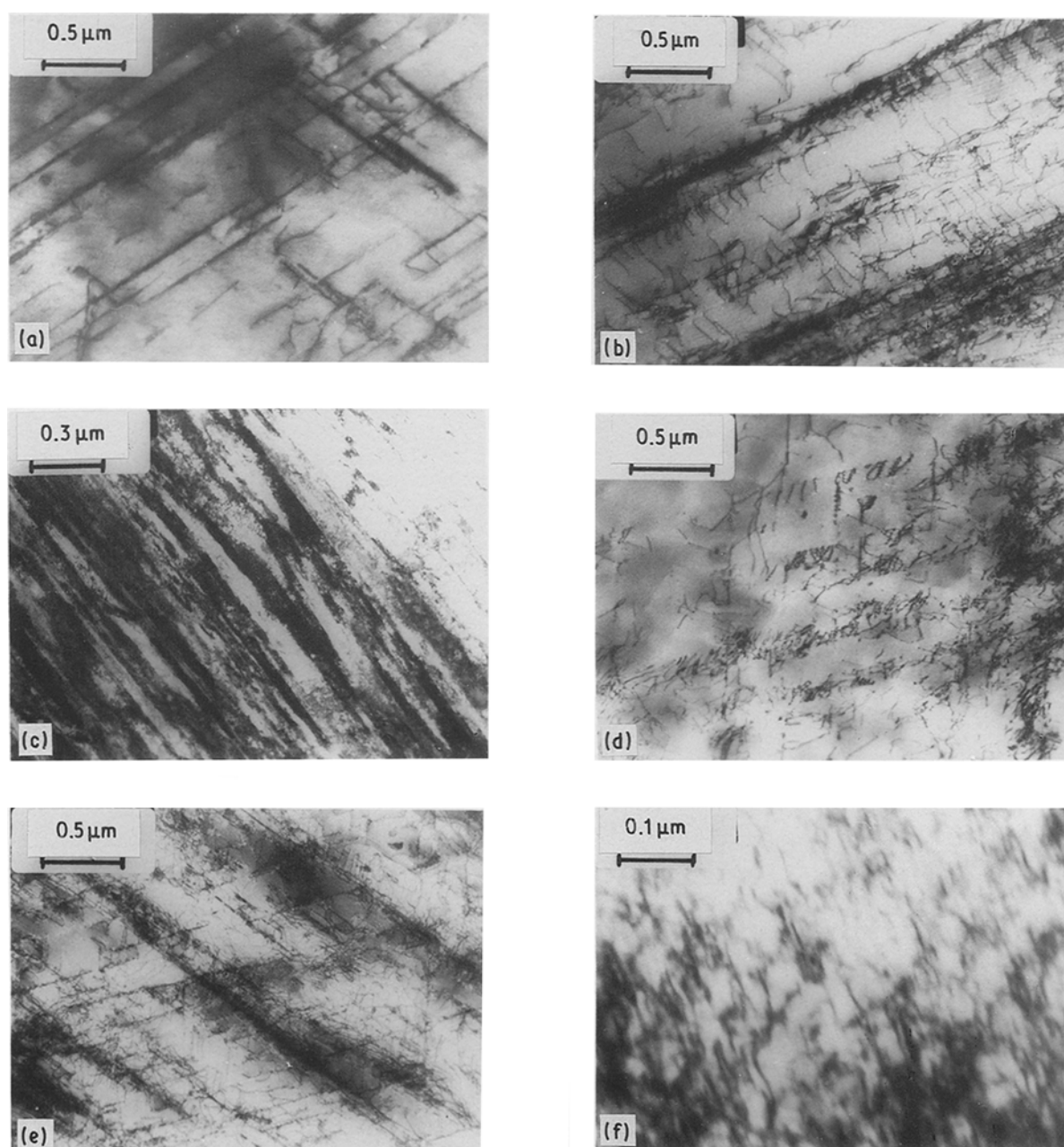


Figure 5 Transmission electron micrographs of the austenite microstructure after different amounts of cold- and warm-deformation: (a)  $\epsilon = 10\%$ ,  $T_\epsilon = \text{RT}$ ; (b)  $\epsilon = 30\%$ ,  $T_\epsilon = \text{RT}$ ; (c)  $\epsilon = 50\%$ ,  $T_\epsilon = \text{RT}$ ; (d)  $\epsilon = 10\%$ ,  $T_\epsilon = 300^\circ\text{C}$ ; (e)  $\epsilon = 30\%$ ,  $T_\epsilon = 300^\circ\text{C}$ ; (f)  $\epsilon = 50\%$ ,  $T_\epsilon = 300^\circ\text{C}$ .

## Acknowledgement

We thank DFG (Ho 325/20-1) for financial support.

## References

1. E. HORNBÖGEN, *Z. Metallkunde* **75** (1984) 741.
2. *Idem*, *Acta Metall.* **33** (1985) 595.
3. *Idem*, *ibid.* **32** (1984) 615.
4. J. F. BREEDIS, *ibid.* **13** (1965) 239.
5. G. ZOUHAR, H. WADEWITZ and A. GÜTH, *Neue Hütte* **28** (1983) 291.
6. M. T. JAHN, Z. M. FAN and C. M. WAN, *J. Mater. Sci.* **20** (1985) 2757.
7. M. HATHERLY, Proceedings of the International Conference on Strength of Metals and Alloys 6, edited by R. C. Gifkins (Pergamon, Oxford, 1982) pp. 1181–95.

*Received 30 September  
and accepted 10 November 1986*